Reaction Kinetics, Mechanisms and Catalysis (2019) 126:341–352
https://doi.org/10.1007/s11144-018-1506-x

Influence of co-fed gases (O_2, CO_2, CH_4, and H_2O) on the N_2O decomposition over (Co, Fe)-ZSM-5 and (Co, Fe)-BETA catalysts

Nayara F. Biturini[1] · Ana Paula N. M. Santos[1] · Marcelo S. Batista[1]

Received: 1 October 2018 / Accepted: 16 November 2018 / Published online: 22 November 2018

Abstract

The influence of co-fed gases (O_2, CO_2, CH_4, and H_2O) on the N_2O decomposition over (Co or Fe)-BETA and (Co, Fe)-ZSM-5 catalysts prepared by ion exchange method was investigated. Co^{2+} ions and oxo dinuclear Co species were identified in Co-ZSM-5 and Co-BETA catalysts. Isolated and oligomeric Fe^{3+} species in cationic sites and Fe_2O_3 particles were found on surface of the Fe-ZSM-5 and Fe-BETA catalysts. Cobalt catalysts were more actives than iron catalysts for the direct decomposition of N_2O. Conversion of N_2O over Fe-BETA and Fe-ZSM-5 was remained stable when co-fed O_2, CO_2, and CH_4, but decreases with water vapor. However, Co-BETA and Co-ZSM-5 showed much larger reaction rate for N_2O decomposition and were very stable when co-fed O_2, CO_2, CH_4, and especially H_2O. The results showed that the higher CH_4 consumption during N_2O reaction over Co-BETA and Co-ZSM-5 was due to CH_4 combustion.

Keywords N_2O decomposition · Co-fed gases · Iron species · Cobalt species · ZSM-5 zeolite · BETA zeolite

Introduction

Nitrous oxide (N_2O) is a potent greenhouse-effect gas with global warming potential (GWP) per molecule of about 300 times and 21 times higher than that of carbon dioxide (CO_2) and methane (CH_4), respectively. Nitrous oxide is not only a greenhouse gas, but also contributes to stratospheric ozone depletion [1–3]. The increase in anthropogenic N_2O emissions (combustion, production of nitric and adipic acids, etc.) shows that the development of effective methods to reduce these emissions is therefore urgent. Consequently, extensive efforts are focused on catalysts for the decomposition of N_2O

✉ Marcelo S. Batista
marcelobatista@ufsj.edu.br

[1] Chemical Engineering Department, Federal University of São João Del Rei, Campus Alto Paraopeba, Rodovia MG 443, Km 5, POBox 131, Ouro Branco, MG CEP 36420-000, Brazil

into harmless N_2 and O_2 due to their efficiency, simplicity and low preparation costs [4, 5].

N_2O decomposition has been evaluated on several catalysts, such as supported noble metals [6–8], transition metal oxides [8–12], and metal exchanged zeolites [13–15]. Noble metal based catalysts as Pt and Rh are active at low temperatures. However, the higher cost of these catalysts and the conversion reduction when co-fed with O_2 and/or H_2O make their industrial application unviable [16]. Additionally, metal oxide based catalysts have been proposed for high temperature operation conditions. However, Liu et al. [8] as well as Yu et al. [17] showed that the N_2O conversion decreases in presence of H_2O, CO_2, and O_2, which are commonly found in industrial exhausts. Recent progress in the N_2O decomposition reaction has been studied with the focus on transition-metal (Cu, Fe, Co)-modified zeolite catalysts [13–15, 18, 19]. Efforts dedicated to Cu-ZSM-5 have shown that decomposition of N_2O is inhibited by O_2 or H_2O co-fed [18]. On the other hand, Fe-zeolite catalysts have been outstanding due to their high activity and resistance in co-fed of CH_4, CO, O_2 and SO_2 [20, 21]. Fe-ZSM-5 has been most studied experimentally and theoretically for the decomposition of N_2O [22, 23]. It is believed that isolated Fe^{3+} and oligonuclear $Fe_x^{3+}O_y$ clusters on the exchanged sites affects the catalytic performance [13, 22]. Furthermore, it is also notable that Co-sites were more active than Fe-sites due to lower activation energy barrier for the direct decomposition of N_2O [19, 24]. According to some authors [13, 20], the activity of (Fe, Co)-zeolite catalysts also depends on the intrinsic properties of each zeolitic structure.

Some studies with BETA zeolite have shown attractive and advantageous characteristics of this material for catalysis, such as: wide pore opening, three-dimensional channel system, large specific area, high thermal and hydrothermal stability and shape selectivity [13, 14]. In terms of the zeolite topology, Fe-BETA was the most effective material between various commercial zeolites (MFI, FER, MOR, FAU) with similar Si/Al ratios for the decomposition of N_2O [25] exhibiting superior activity in comparison with Fe-ZSM-5 [26]. Additionally, Liu et al. [19] reported that the activity of Co-BETA was higher than that of Fe- or Cu-BETA comparing by the turnover frequency (TOF).

Although some studies for N_2O decomposition by using beta-type zeolites has been done as previously reported [19, 25, 26], these works were not done with co-fed gases commonly found in industrial emissions. In addition, the performance of cobalt-containing zeolites for N_2O decomposition is so far not well established. Therefore, the objective of this work was to study the influence of co-fed O_2, CO_2, H_2O and CH_4 on the direct decomposition of N_2O over (Co, Fe)-BETA and (Co, Fe)-ZSM-5 catalysts. These catalysts were prepared by ion exchange method and its characterization using XRD, H_2-TPR and UV–VIS spectroscopy was also discussed.

Materials and methods

Catalyst preparation

The (Co, Fe)-ZSM-5 and (Co, Fe)-BETA catalysts were prepared by ion-exchange methods using commercial Na-ZSM-5 (ALSI-PENTA Zeolithe Gmbh)

and NH_4-BETA (TRICAT) zeolites with similar Si/Al molar ratios. The parent zeolite (3 g) was added to 1 mol/L aqueous solutions (150 mL) of iron nitrate ($Fe(NO_3)_3{\cdot}9H_2O$) and cobalt nitrate ($Co(NO_3)_2{\cdot}6H_2O$) at 50 °C. The mixture was vigorously stirred for 12 h. The sample was exchanged three times under the same conditions. Between each ion-exchange, the mixture was filtered; the solid was washed with distilled water and dried at 110 °C. Finally, the (Co, Fe)-ZSM-5 and (Co, Fe)-BETA catalysts were obtained after further calcination in muffle oven at 650 °C for 2 h under static air.

Catalyst characterization

The catalysts were characterized by X-ray diffraction (XRD), temperature programmed reduction with H_2 (H_2-TPR) and UV–Visible Diffuse Reflectance Spectroscopy (UV–VIS). XRD analyzes were performed by the powder method using a Rigaku diffractometer (Miniflex 600) with Cu tube, Ni-filtered, operating at 40 kV, 15 mA and Cu K_α radiation. The speed of the goniometer used was 2° (2θ)/min, the angle ranging between 5 and 80° (2θ). The crystal phases were determined by correlating the diffraction patterns with those in the X'Pert HighScore reference.

H_2-TPR analyses were performed on SAMP3 apparatus (Termolab Equipment, Brazil) equipped with a thermal conductivity detector (TCD). A trap was used to remove the water stemming from the reduction before the gas of the reactor outlet was sent to the TCD. TPR started with a ramp of 10 °C/min from 100 °C until 1000 °C. A flow of 30 mL/min from a high purity mixture of 2 V % H_2 in Ar was used.

UV–VIS analyses were carried out in an Ocean Optics USB2000 spectrometer using a quartz cell. Before the measurement, the samples were dried at 120 °C for 2 h to remove the water molecule or OH groups. Samples were scanned in the range of 200–800 nm. The reflectance data were converted to the Schuster–Kubella–Munk function, $F(R) = (1-R)^2/2R$, where R is the diffuse reflectance obtained directly from the spectrometer.

Catalytic activity

Catalytic tests for N_2O decomposition over (Co, Fe)-ZSM-5 and (Co, Fe)-BETA catalysts were carried out in U-shaped quartz reactor with an inner diameter of 9 mm. An electric furnace equipped with PID temperature control was used to heat the reactor. About 40 mg of catalyst were placed on fixed bed of quartz-wool inside the reactor. For all the experiments, 60 mL/min from a mixture of 10 V % N_2O in He was flowed continuously into the reactor, corresponding to a GHSV of 30,000 h^{-1}. Catalytic performance started with a ramp of 10 °C/min from 25 to 600 °C. The effect of co-fed gases on catalytic performance of catalysts was studied by adding 10 V % O_2, 10 V % CO_2, 10 V % CH_4 and 10 V % H_2O vapor (by saturator) into the reaction mixture at 600 °C whereas the concentration of N_2O was still 10 V %, and the total flow of the gas was still 60 mL/min. The gaseous mixture flows were adjusted by electronic controllers (Brooks Instrument 0254).

The reactor was coupled in line to mass spectrometer (Pfeiffer Vacuum, ThermoStar GSD 320T) for gas analysis: N_2 ($m/z = 28$), O_2 ($m/z = 32$), N_2O ($m/z = 44$ and 30), CH_4 ($m/z = 16$ and 15), CO_2 ($m/z = 44$) and He ($m/z = 4$). The conversion of nitrous oxide was calculated through Eq. 1.

$$\text{Conversion of } N_2O\ (\%) = \left(\frac{N_2O_{(in)} - N_2O_{(out)}}{N_2O_{(in)}} \right) \times 100\% \quad (1)$$

where $[N_2O]_{in}$ refers to molar flow of N_2O at room temperature, and $[N_2O]_{out}$ refers to molar flow of N_2O at an elevated temperature. The reaction rate was calculated as mol of N_2O converted per hour/total mol of Fe or Co (measured by XRF), using conditions of kinetic regime, temperature established and catalytic activity stable [27, 28].

Results and discussion

Fig. 1 shows the XRD patterns of the ZSM-5 and BETA zeolites and also of the (Co, Fe)-ZSM-5 and (Co, Fe)-BETA catalysts. The MFI and BEA crystalline structures were well preserved even after exchange with Fe or Co ions. (Co, Fe)-ZSM-5 catalysts showed characteristics peaks of precursor ZSM-5 zeolite in $2\theta = 7.8°$, 8.7°, 15.7°, 23.0°, 23.7°, 29.7°, 45.1° (PDF 37-0359). In its turn, (Co, Fe)-BETA catalyst showed characteristics peaks of BETA-typed zeolite in $2\theta = 7.6°$, 22.3° (PDF 48-0074). Close examination of Fig. 1 shows slight reductions in the peak intensities of the Fe-ZSM-5 and Fe-BETA catalysts due to the higher X-ray absorption coefficient of Fe compounds [29, 30]. No diffraction

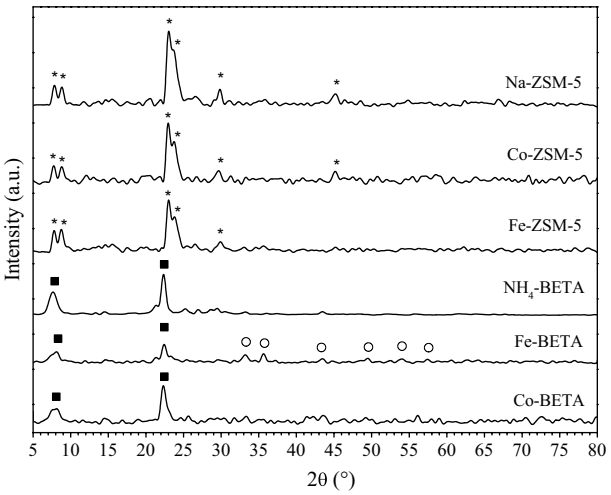

Fig. 1 XRD patterns of ZSM-5 and BETA zeolites and (Co, Fe)-ZSM-5 and (Co, Fe)-BETA catalysts. Typical peaks of: (asterisk) ZSM-5, (filled square) BETA and (open circle) Fe_2O_3

peaks from FeO_x nanoparticles were observed for Fe-ZSM-5 evidencing only the presence of Fe-exchanged active species in the zeolite structure. However, the existence of tiny FeO_x species cannot be totally excluded as considering their amounts are possibly below the XRD detection limit. On the other hand, Fe-BETA shows characteristic peaks of Fe_2O_3 in $2\theta = 33.2°$, 35.6°, 40.9°, 49.5°, 54.1°, 62.5°, 64.1° (PDF 01-1053). The absence of Co_3O_4 peaks in Co-ZSM-5 and Co-BETA diffractograms indicates the presence of Co-exchanged species in the zeolite structure. In view of the solubility, the precipitation of $Fe(OH)_3$ ($K_{SP} = 2.7 \times 10^{-39}$, 25 °C) is more thermodynamically expected than $Co(OH)_2$ ($K_{SP} = 5.9 \times 10^{-15}$, 25 °C) for our catalysts. However, the preparation conditions (low pH and temperature at 50 °C) used in this work appear to have prevented further formation of cobalt oxides.

Fig. 2 shows the TPR profiles of (Co, Fe)-ZSM-5 and (Co, Fe)-BETA catalysts. No reduction peaks were observed in profiles of Co-ZSM-5 and Co-BETA, confirming the absence of cobalt oxides on surface of these catalysts. These results are also consistent with the XRD measurement. Most Co species exist in the form of Co^{2+} at the ion exchange sites and the further reduction of Co^{2+} into Co^0 occurred above 1000 °C [31]. As seen from Fig. 2, the first two peaks (347 and 537 °C) of Fe-BETA and the peak at 334 °C of Fe-ZSM-5 were mainly assigned to reduction of Fe^{3+} to Fe^{2+} (in cations or oxo-cations) [32]. Fe-ZSM-5 and Fe-BETA catalysts showed a slight shoulder at 640 and 690 °C, respectively, which were attributed to the reduction of FeO to Fe^0 [19, 26], confirming that trace amount of Fe_2O_3 aggregated on zeolite surface. It has been reported that, the corresponding H_2 consumption of Fe_2O_3 to FeO was actually comprised in the former two peaks of Fe-BETA and together with the first Fe-ZSM-5 peak [26]. Further reduction of Fe^{2+} into Fe^0 was not observed under the conditions used, it usually occurred above 1000 °C and causes the collapse of the zeolite structure [33]. In general, Co- and Fe-exchanged sites with the zeolite framework were

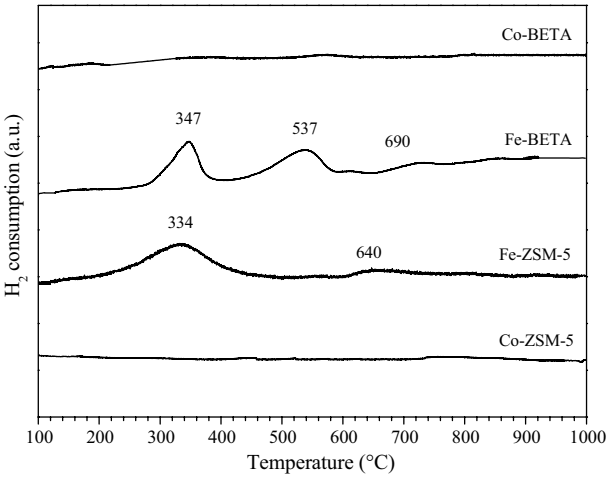

Fig. 2 H_2-TPR profiles of (Co, Fe)-ZSM-5 and (Co, Fe)-BETA catalysts

predominant in the (Co, Fe)-ZSM-5 and (Co, Fe)-BETA catalysts. These cationic species are known as the most active sites for the direct decomposition of nitrous oxide.

The further information on the cobalt and iron species present in the (Co, Fe)-ZSM-5 and (Co, Fe)-BETA catalysts were studied by UV–VIS spectroscopy, as shown in Fig. 3. Co-BETA (Fig. 3a) and Co-ZSM-5 (Fig. 3b) showed a band located at 200–235 nm corresponding to transitions from the oxygen atoms to Co^{2+} ions in the cationic sites, and a band of the ligand to metal $O \rightarrow Co^{2+}$ charge-transfer of the -oxo dinuclear Co species at 240–350 nm and broad absorption in the region of d–d transitions at 360–750 nm of the octahedral Co^{2+} ions in ion-exchange position, according to the literature reports [34–36]. Wichterlová et al. [37, 38] assigned the bands in the visible range to Co^{2+} located at three different sites in the ZSM-5 and BETA, i.e., α- (680 nm), β- (460, 570, 613, 645 nm) and γ-sites (497 and 540 nm). In addition, both cobalt-catalysts are light pink in color, typical of the presence of $[Co(II)(H_2O)_6]^{2+}$ compensating the negative charge of the zeolite framework. These results are consistent with the XRD and TPR measurements of these catalysts.

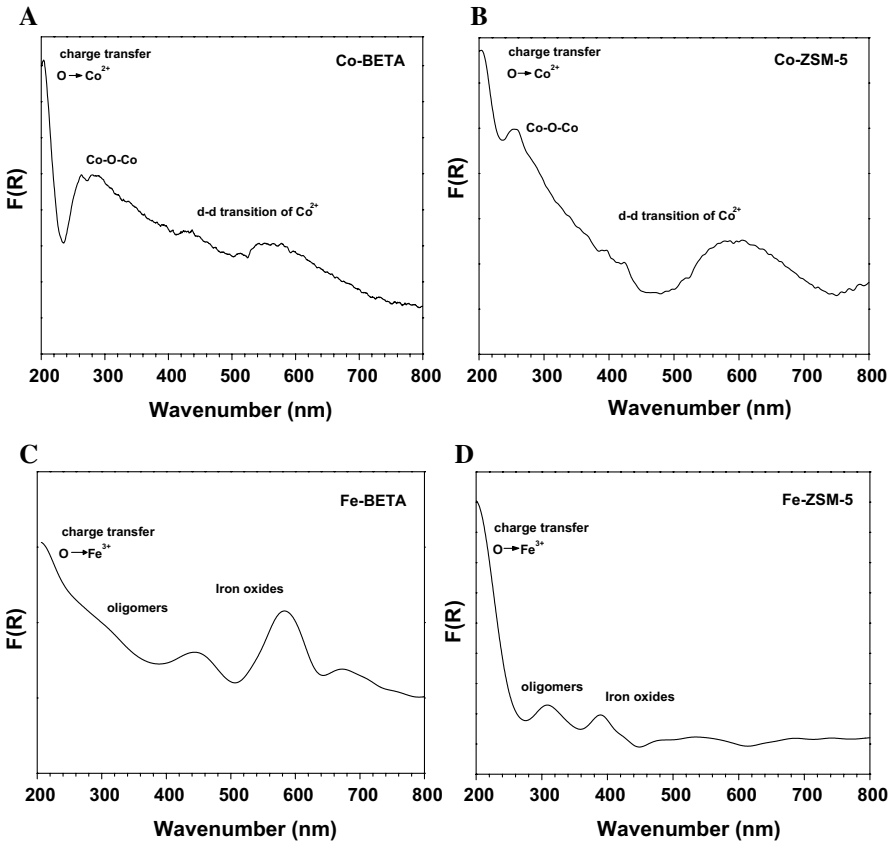

Fig. 3 UV–VIS spectra of: **a** Co-BETA, **b** Co-ZSM-5, **c** Fe-BETA and **d** Fe-ZSM-5

As for the UV–VIS spectra of Fe-BETA (Fig. 3c) and Fe-ZSM-5 (Fig. 3d), the two bands observed at 200–260 nm and at 260–360 nm corresponding to the typical ligand to metal charge transfer (LMCT) bands of isolated Fe^{3+} species in the cationic sites [19, 34] and isolated or oligomeric extraframework Fe species in zeolite channels [22], respectively. The bands at 360–460 nm (iron oxide clusters) and > 450 nm (large surface oxide species) can be associated to Fe_2O_3 particles on zeolite surface [22]. Note that the spectrum of the Fe-ZSM-5 catalyst was characterized by a low intensity absorption edge at 550 nm reflecting low concentration of Fe oxide nanoparticles, which was not detected by XRD (< 4 nm), however observed by TPR. On the other hand, Fe-BETA showed a significant increase of the band above 500 nm confirming the present of large particles of Fe_2O_3 on zeolite surface, as already commented by XDR and TPR.

Fig. 4 shows the N_2O conversions on (Co, Fe)-BETA and (Co, Fe)-ZSM-5 catalyst as a function of reaction temperature. It was found that the N_2O conversion rises very rapidly with the temperature on Co-ZSM-5 and Co-BETA, but much more smoothly on Fe-ZSM-5 and Fe-BETA. Co-species might be well dispersed as an ionic form, as verified by H_2-TPR, leading to increase of N_2O conversion. Therefore, cobalt-based catalysts were more actives than iron-based catalysts showing that cobalt species in ion-exchange position are more actives due to lower activation energy barrier for the direct decomposition of N_2O. Considering that the actual metal loads of Co-BETA (3.4%), Co-ZSM-5 (3.2%) Fe-BETA (6.5%) and Fe-ZSM-5 (0.3%) were different; the activities were compared by reaction rate. Results of the reaction rate calculation at 450 °C also showed that Co-BETA (14.2 h^{-1}) and Co-ZSM-5 (12.0 h^{-1}) were more effective catalysts than Fe-BETA (1.9 h^{-1}) and Fe-ZSM-5 (3.0 h^{-1}). In addition, the reaction rates of our cobalt-zeolite catalysts were much higher than those of cobalt oxides (≤ 1 h^{-1}) [39–41]. The reaction rates (called TOF) of Fe zeolite catalysts (BEA, FAU, MOR, FER) reported in the literature, are in the range 0.03–7.11 h^{-1} at 400–500 °C, depending critically on the preparation/

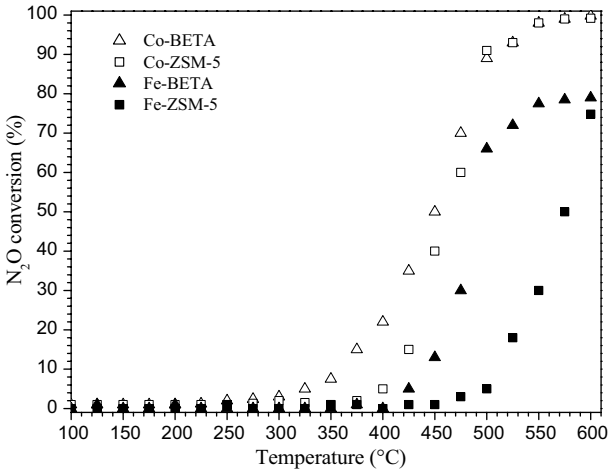

Fig. 4 N_2O decomposition over (Co, Fe)-BETA and (Co, Fe)-ZSM-5 catalysts

pretreatment [23]. Therefore, the activity of our Fe-BETA and Fe-ZSM-5 catalysts is within the range of reaction rates found in the literature. As for the Co-catalysts, the reaction rate was comparable to those values reported in the literature [42, 43]. Reaction rate discrepancies of the previous and present works are mainly attributed to the different reaction conditions such as the m_{cat}, GHSV, and especially for the N_2O concentrations [19] and also the catalyst preparation [42].

As noted, the nature of the host zeolite has a great influence on the reactivity of Fe and Co species with respect to N_2O. Co-BETA was the most active material at low temperatures. This can be understood to both the large amount of active sites and to the widely open porosity of the BEA structure. Co-BETA and Co-ZSM-5 catalysts show similar conversions at higher temperatures due to the mass transfer regime. However, it is known that the decomposition of N_2O over catalysts is inhibited mainly by O_2 or H_2O co-fed. The inhibiting effect of O_2 and H_2O vapor has been attributed to the competition adsorption between N_2O and O_2 or H_2O [16, 19] and hydroxylation of the active sites by H_2O [23, 44].

Fig. 5 shows that the conversion of N_2O over Fe-BETA and Fe-ZSM-5 practically remained stable in the presence of O_2, CO_2, and CH_4, but decreases slightly (~6%) was observed in the presence of water vapor. This deactivation in the presence of H_2O was associated with the hydroxylation of the active iron sites [23, 44]. The effect of periodic step changes of co-fed 10 vol% of O_2, CO_2, CH_4 and H_2O, on the performance of over Co-BETA and Co-ZSM-5 at 600 °C are shown in Fig. 6. The N_2O conversion was about 99% without co-fed (no shown), consistent with the value seen in Fig. 4. Note that the N_2O conversion over Co-BETA and Co-ZSM-5 was maintained after the introduction of 10 V% O_2 and 10 V% CO_2. In the presence of H_2O, no significant change was observed in the conversion of N_2O to both catalysts. These results indicated that cobalt sites were more resistant to hydroxylation than the iron sites exchanged in BETA and ZSM-5 zeolites. The N_2O conversion over

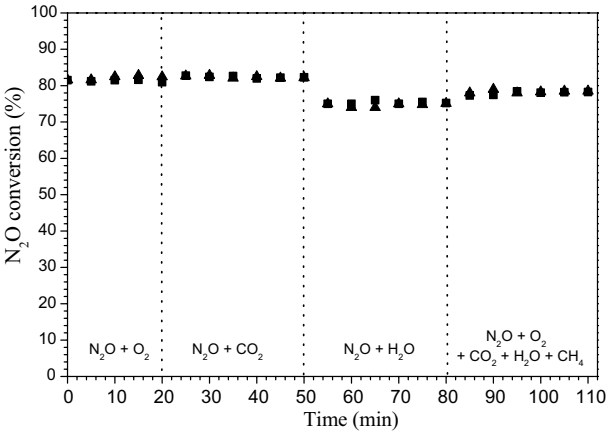

Fig. 5 Effect of co-fed gases on the N_2O conversion over Fe-BETA (filled triangle) and Fe-ZSM-5 (filled square) catalysts. Condition: reaction at 600 °C and gas mixture: 10% N_2O, 10% O_2, 10% CO_2, 10% CH_4, 10% H_2O and inert balance

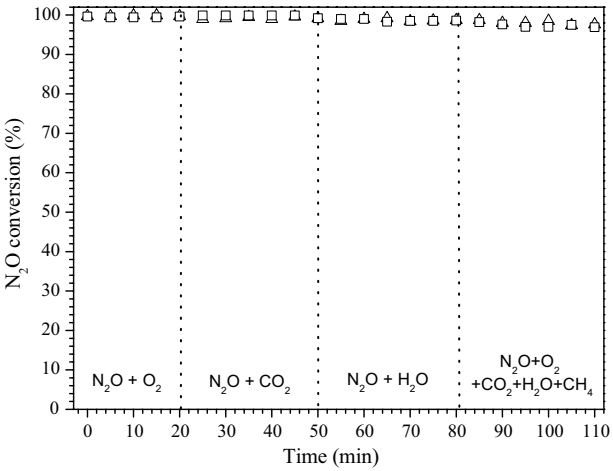

Fig. 6 Effect of co-fed gases on the N_2O conversion over Co-BETA (open triangle) and Co-ZSM-5 (open square) catalysts. Condition: reaction at 600 °C and gas mixture: 10% N_2O, 10% O_2, 10% CO_2, 10% CH_4, 10% H_2O and inert balance

Co-BETA and Co-ZSM-5 was also maintained after the introduction of all gases (O_2, CO_2, CH_4 and H_2O). In general, Co-BETA and Co-ZSM-5 are highly actives for the N_2O decomposition, showing reaction rate clearly much larger and, interestingly, are very stable in the presence of O_2, CO_2, CH_4, and especially H_2O, with a slight decay of conversion of 0.06%/h.

Methane is also a greenhouse gas that must be eliminated from the stream of effluent gases. For this purpose, the methane consumption was monitored during the N_2O reaction. Fig. 7 shows the CH_4 conversion over Co-BETA and Co-ZSM-5 catalysts during N_2O reaction at 600 °C co-fed with complete gas mixture ($N_2O + CH_4 + O_2 + CO_2 + H_2O$). Note that CH_4 consumption occurs on both cobalt-catalysts; however, Co-ZSM-5 consumes more CH_4 than Co-BETA. It is known that the apparent activation energy for N_2O reduction by CH_4 is very similar to that of direct N_2O decomposition (140 kJ/mol) [20]. In the case of N_2O reduction by methane (Eq. 2), the stoichiometric amount requires to 1 mol of CH_4 to reduce 4 mol of N_2O, i.e. maximum methane conversion of 25%. Thus, the higher methane consumption on Co-BETA (70%) and Co-ZSM-5 (92%) must be associated with the occurrence of CH_4 combustion reaction (Eq. 3).

$$CH_4 + 4N_2O \rightarrow 4N_2 + CO_2 + 2H_2O \quad (2)$$

$$CH_4 + 2O_2 \rightarrow CO_2 + 2H_2O \quad (3)$$

Our observations suggest that the reactions of N_2O decomposition and reduction of N_2O by CH_4 proceed via different reaction mechanism and might occur over cobalt sites of the zeolite. Nobukawa et al. [45] measured the oxidation rates of methane with N_2O and O_2, and found that the intermediates of methoxy were oxidized with N_2O more rapidly than O_2. However, our results showed that the co-fed

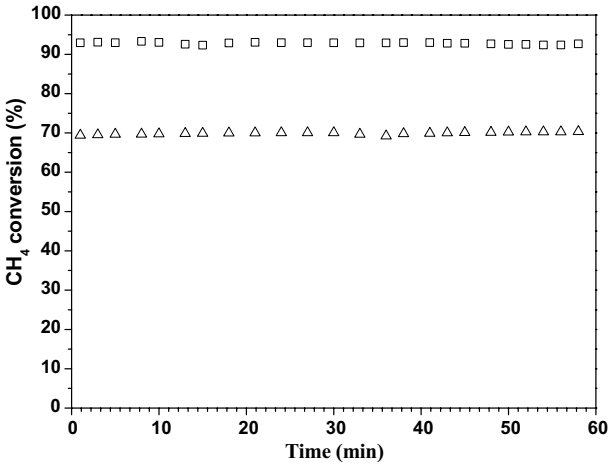

Fig. 7 CH_4 conversion over Co-BETA (open triangle) and Co-ZSM-5 (open square) during N_2O reaction at 600 °C co-fed with complete gas mixture ($N_2O + CH_4 + O_2 + CO_2 + H_2O$)

with complete gas mixture ($N_2O + CH_4 + O_2 + CO_2 + H_2O$) did not change the N_2O conversion over Co-BETA and Co-ZSM-5 catalysts.

Conclusions

(Co, Fe)-BETA and (Co, Fe)-ZSM-5 catalysts prepared by ion-exchange method have Co^{2+} ions, and oxo dinuclear Co species or isolated and oligomeric Fe^{3+} species compensating the negative charge of the zeolite framework, as shown by UV–VIS spectroscopy. In addition, Fe_2O_3 particles were found on surface of the Fe-ZSM-5 and Fe-BETA catalysts. Cobalt-catalysts were more actives than iron-catalysts for the direct decomposition of N_2O. Conversion of N_2O over Fe-BETA and Fe-ZSM-5 practically remained stable in the presence of O_2, CO_2, and CH_4, but decreases slightly in the presence of water vapor. On the other hand, Co-BETA and Co-ZSM-5 were highly actives for the N_2O decomposition, showing reaction rate clearly much larger and, interestingly, were very stable in the presence of O_2, CO_2, CH_4, and especially H_2O, with a slight decay of conversion of 0.06%/h. The higher CH_4 consumption during N_2O reaction on Co-BETA (70%) and Co-ZSM-5 (92%) was due to CH_4 combustion.

Acknowledgements The authors would like to acknowledge FAPEMIG (TEC-APQ-03361-15) for financial support of this research and Nayara Fernandes Biturini is grateful to the CAPES (Brazil) for a scholarship.

References

1. Zhang X, Guan Y, Zhang S, Yang M, Zhao Y, Hao Z (2014) J Mol Catal A 395:202–209
2. IPCC (2013) Climate Change 2013: the physical science basis. Contribution of working group I to the Fifth Assessment Report of the Intergovernmental Panel on Climate Change
3. Frutos OD, Quijano G, Aizpuru A, Muñoz R (2018) Biotechnol Adv 36:1025–1037
4. Wu M, Wang H, Zhong L, Zhang X, Hao Z, Shen Q, Wei W, Qian G, Sun Y (2016) Chin J Catal 37:898–907
5. Melián-Cabrera I, Espinosa S, Mentruit C, Murray B, Falco L, Socci J, Kapteijn F, Moulijn JA (2018) Ind Eng Chem Res 57(3):939–945
6. Parres-Esclapez S, Illán-Gómez MJ, Lecea CS, Bueno-López A (2010) Appl Catal B 96:370
7. Pachatouridou E, Papista E, Iliopoulou EF, Delimitis A, Goula G, Yentekakis IV, Marnellos GE, Konsolakis M (2015) J Environ Chem Eng 3:815
8. Liu Z, He F, Ma L, Peng S (2016) Catal Surv Asia 20(3):121–132
9. Pietrogiacomi D, Campa MC, Carbone LR, Tuti S, Occhiuzzi M (2016) Appl Catal B 187:218–227
10. Wang J, Feng M, Zhang HJ, Xu XF (2014) J Fuel Chem Technol 42:1464–1469
11. Zhou H, Huang Z, Sun C, Qin F, Xiong D, Shen W, Xu H (2012) Appl Catal B 125:492
12. Zabilskiy M, Djinović P, Tchernychova E, Tkachenko OP, Kustov LM, Pintar A (2015) ACS Catal 5:5357
13. Wang J, Xia H, Ju X, Fan F, Feng Z, Li C (2013) Chin J Catal 34:876–888
14. Sklenak S, Andrikopoulos PC, Boekf B, Jansang B, Nováková J, Benco L, Bucko T, Hafner J, Dědeček J, Sobalík Z (2010) J Catal 272:262–274
15. Moura APN, Batista MS (2017) Matéria. https://doi.org/10.1590/s1517-707620170003.0190
16. Lin Y, Meng T, Ma Z (2015) J Ind Eng Chem 28:138
17. Yu H, Tursun M, Wang X, Wu X (2016) Appl Catal B 185:110–118
18. Meng T, Ren N, Ma Z (2015) J Mol Catal A 404:233–239
19. Liu N, Zhang R, Chen B, Li Y, Li Y (2012) J Catal 294:99–112
20. Debbagh MN, Lecea CSM, Pérez-Ramírez J (2007) Appl Catal B 70:335–341
21. Pérez RJ, Kapteijn F, Mul G, Moulijn JA (2002) Appl Catal B 35(3):227–234
22. Richards N, Nowicka E, Carter JH, Morgan DJ, Dummer NF, Golunski S, Hutchings GJ (2018) Top Catal. https://doi.org/10.1007/s11244-018-1024-0
23. Xie P, Luo P, Ma Z, Huang C, Miao C, Yue Y, Hua W, Gao Z (2015) J Catal 330:311–322
24. Ryder JA, Chakraborty AK, Bell AT (2002) J Phys Chem B 106(28):7059–7064
25. Øygarden AH, Pérez-Ramírez J (2006) Appl Catal B 65(1–2):163–167
26. Chen B, Liu N, Liu X, Zhang R, Li Y, Li Y, Sun X (2011) Catal Today 175(1):245–255
27. Lente G (2013) ACS Catal 3(3):381–382
28. Bligaard T, Bullock RM, Campbell CT, Chen JG, Gates BC, Gorte RJ, Jones CW, Jones WD, Kitchin JR, Scott SL (2016) ACS Catal 6(4):2590–2602
29. Jouini H, Mejri I, Martinez-Ortigosa J, Cerrillo JL, Mhamdi M, Palomares AE, Delahay G, Blasco T (2018) Solid State Sci 84:75–85
30. Qi G, Yang RT (2005) Appl Catal A 287(1):25–33
31. Jong SJ, Cheng S (1995) Appl Catal A 126(1):51–66
32. Guzmán-Vargas A, Delahay G, Coq B (2003) Appl Catal B 42(4):369–379
33. Feng XD, Hall WK (1997) J Catal 166:368–376
34. Sazama P, Pilar R, Mokrzycki L, Vondrova A, Kaucky D, Plsek J, Sklenak S, Stastny P, Klein P (2016) Appl Catal B 15(189):65–74
35. Beznis NV, Weckhuysen BM, Bitter JH (2010) Catal Lett 136(1–2):52–56
36. Castilho S, Borrego A, Henriques C, Ribeiro MF, Fernandes A (2017) Inorg Chim Acta 455:568–574
37. Dědeček J, Čapek L, Kaucký D, Sobalık Z, Wichterlova B (2002) J Catal 211(1):198–207
38. Sazama P, Tabor E, Klein P, Wichterlova B, Sklenak S, Mokrzycki L, Pashkkova V, Ogura M, Dedecek J (2016) J Catal 333:102–114
39. Jirátová K, Kovanda F, Balabánová J, Koloušek D, Klegová A, Pacultová K, Obalová L (2017) Reac Kinet Mech Cat 121(1):121–139
40. Ciura K, Grzybek G, Wójcik S, Indyka P, Kotarba A, Sojka Z (2017) Reac Kinet Mech Cat 121(2):645–655
41. Wang Y, Hu X, Zheng K, Zhang H, Zhao Y (2018) Reac Kinet Mech Cat 123(2):707–721
42. Zhang X, Shen Q, He C, Ma C, Cheng J, Liu Z, Hao Z (2012) Catal Sci Technol 2(6):1249–1258

43. Smeets PJ, Meng Q, Corthals S, Leeman H, Schoonheydt RA (2008) Appl Catal B 84(3–4):505–513
44. Rutkowska M, Piwowarska Z, Micek E, Chmielarz L (2015) Microporous Mesoporous Mater 209:54–65
45. Nobukawa T, Yoshida M, Kameoka S, Ito SI, Tomishige K, Kunimori K (2004) J Phys Chem B 108(13):4071–4079